

Toward terahertz heterodyne detection with superconducting Josephson nano-junctions

A. Luo¹, T. Wolf¹, Y. Wang¹, M. Malnou¹, C. Ulysse², G. Faini², P. Febvre³, M. Sirena⁴, J. Lesueur¹, N. Bergeal¹

¹*Laboratoire de Physique et d'Etude des Matériaux - UMR8213-CNRS,*

ESPCI ParisTech, 10 Rue Vauquelin - 75005 Paris, France.

²*Laboratoire de Photonique et de Nanostructures LPN-CNRS, Route de Nozay, 91460 Marcoussis, France.*

³*IMEP-LAHC - UMR 5130 CNRS, Université de Savoie, 73376 Le Bourget du Lac cedex, France. and*

⁴*Centro Atómico Bariloche, Instituto Balseiro CNEA and Univ. Nac. de Cuyo,*

Av. Bustillo 9500, 8400 Bariloche, Rio Negro Argentina.

(Dated: November 2, 2021)

In this letter, we present the study of the high-frequency mixing properties of ion irradiated $\text{YBa}_2\text{Cu}_3\text{O}_7$ Josephson nano-junctions. The frequency range, spanning above and below the characteristic frequencies f_c of the junctions, permits a clear observation of the transition between two mixing regimes. The experimental conversion gain was found to be in good agreement with the prediction of the three ports model. Finally, we discuss the potential of the junctions to build a Josephson mixer operating in the terahertz frequency range.

The terahertz (THz) region of the electromagnetic spectrum [0.3-10THz] has, so far, not been exploited fully due to the lack of suitable sources and detectors [1]. Indeed, THz frequency lies between the frequency range of traditional electronics and photonics where the existing technology cannot be simply extended. Low temperature superconducting-insulating-superconducting Niobium tunnel junctions are currently used as frequency mixing element in heterodyne receivers [2], providing extremely low noise and high sensitivity [3]. However, they are intrinsically limited in frequency by the energy gap of Nb (~ 800 GHz) and operate only at low temperature (4.2K).

An alternative to these devices consists of using high-temperature superconducting (HTS) receivers based on Josephson Junctions mixers or hot-electron bolometers. In addition to the obvious advantage of a much higher operating temperature, the investigation of HTS mixers is motivated by the possibility of approaching quantum-limited noise performance at frequencies higher than what is possible with conventional Nb devices [4, 5]. Hence, it is important to develop HTS devices and related heterodyne mixer technology for applications in the THz range. However, despite a few promising realizations mainly based on grain-boundary or ramp edge junctions [6–8], the development was slowed down by the difficulty to build a junction technology sufficiently reliable to fabricate complex

devices. Over the past years, a new approach based on ion irradiation has been developed to make Josephson nano-junctions with high temperature superconductors. This method has been used to make reproducible junctions [9, 10], SQUIDs [11] and large scale integrated Josephson circuits [12, 13]. In this Letter, we present a study of the high-frequency mixing properties of Josephson nano-junctions made by this technique.

Fig 1a shows an optical picture of a Josephson junction embedded in a self-complementary THz spiral antenna. We used 70 nm thick $\text{YBa}_2\text{Cu}_3\text{O}_7$ films grown on sapphire substrates. The junction is defined in a 2 μm wide superconducting channel by irradiating through a 20 nm wide slit with 100 keV oxygen ions at a fluence of 3×10^{13} at/cm². The fabrication method has been described in detail in reference [14]. The junction is connected to contact pads for dc biasing and to a microwave transmission line to read the output signal. The back side of the sapphire substrate is placed in contact with a silicon hyper-hemispheric lens located at the focal point of a parabolic mirror exposed to external signals through the window of the cryostat. The output signal at intermediate frequency is amplified by a cryogenic HEMT amplifier [4-8GHz] before further amplification at room temperature. An isolator is placed in the chain to minimize the back-action of the amplifier on the Josephson mixer.

The resistance of the junction as a function of temperature is shown in figure 1b. The highest transition refers to the superconducting transition of the reservoirs (i.e. non irradiated electrodes) at $T_c^0 = 85$ K, which corresponds to the transition temperature of the unprocessed $\text{YBa}_2\text{Cu}_3\text{O}_7$ film [9]. The second transition at the lower temperature $T_J = 68$ K corresponds to the occurrence of the Josephson coupling between the two electrodes, and not to the transition of the irradiated part itself which is expected at the lower temperature $T_c' \approx 52$ K. Junctions fabricated by this method are in the low capacitance regime, defined by a McCumber dimensionless parameter $\beta_c = \frac{2e}{h} I_c R_n^2 C$ much smaller than one [15] (I_c is the critical current, R_n the normal-state resistance and C the capacitance of the junction). Junctions have non-hysteretic current-voltage characteristics with an upward curvature of the dissipation branch and no sharp feature at the gap voltage (fig1b inset), a behavior well described by the Resistively Shunted Junction (RSJ) model [15].

Below T_J , the critical current I_c increases with a quadratic law when the temperature is lowered (fig1b). At the lower temperature T_c' , the junction enters a flux-flow regime and the I(V) characteristics display a downward curvature (inset fig1b). The characteristic frequency f_c of the junction is defined by the $I_c R_n$ product via the Josephson frequency $f_c = (2e/h) I_c R_n$. Although the mixing operation is optimal when the signal frequency is lower than f_c , it can be performed up to frequencies corresponding to several times the value of f_c with a reduced conversion

efficiency. As can be seen in fig 1b, the characteristic frequency of the nano-junction is temperature-dependent and takes a maximum value $f_c^{\max} = 75\text{GHz}$ at 58K. The decrease of f_c below this temperature is due to the drop of R_n as it approaches the flux flow regime.

The observation of Shapiro steps is important to evaluate the dynamic properties of a Josephson junction [16]. I(V) characteristics under 20GHz radiation have been measured as a function of radiation power. Figure 2a shows the differential resistance of the junction $\frac{dV}{dI}$ as a function of bias current and power radiation. The oscillations of several Shapiro steps with power can be clearly observed here. The data are in qualitative agreement with the predictions of the current driven RSJ model which admits a single parameter f_c (figures 2b and 2c).

To study the mixing properties of the junction, a strong local oscillator signal at frequency f_{LO} and a weaker test signal at frequency f_s are injected through the optical window of the cryostat. Three different ranges of frequency have been investigated : (i) $f_{\text{LO}} = 20\text{GHz} < f_c^{\max}$, (ii) $f_{\text{LO}} = 70\text{GHz} \approx f_c^{\max}$ and (iii) $f_{\text{LO}} = 140\text{GHz} > f_c^{\max}$. Figure 3 shows the output power measured at the intermediate frequency (IF) $f_{\text{IF}} = |f_{\text{LO}} - f_s| = 5.5\text{GHz}$ as a function of the dc voltage V across the junction. In these measurements, the power of the local oscillator has been set to reduce the critical current to approximately half of its value as it corresponds to an optimal operation point for mixer performances. In the regime $f_{\text{LO}} < f_c^{\max}$, the power at f_{IF} displays maximums located at the center of each Shapiro step whereas in the regime $f_{\text{LO}} > f_c^{\max}$ there are two maximums within a Shapiro step, separated by a dip at the center. The regime $f_{\text{LO}} \approx f_c^{\max}$ corresponds to an intermediate situation where the power at f_{IF} is approximately flat at the center of the steps. Mixing at frequency higher than 140 GHz was not investigated in this study.

The three ports model has been used in the context of the RSJ model to calculate the theoretical performance of the mixer [4, 17]. It describes the linear response due to a small signal by solving the non-linear response of the mixer to the local oscillator illumination. Only three frequencies of relevance are considered: the upper side-band (USB) $f_{\text{LO}} + f_{\text{IF}}$, the lower side-band (LSB) $f_{\text{LO}} - f_{\text{IF}}$ and f_{IF} . The frequency conversion matrix is defined by

$$\begin{pmatrix} V_u \\ V_0 \\ V_l^* \end{pmatrix} = \begin{pmatrix} Z_{uu} & Z_{u0} & Z_{ul} \\ Z_{0u} & Z_{00} & Z_{0l} \\ Z_{lu} & Z_{l0} & Z_{ll} \end{pmatrix} \begin{pmatrix} I_u \\ I_0 \\ I_l^* \end{pmatrix}$$

where the $u, l, 0$ stand for USB, LSB and IF respectively, and V_j and I_i are the voltages and currents at those respective frequencies. Each element Z_{ij} is simply the ratio of the voltage at the relevant frequency V_j with the current

injected I_j . The diagonal elements are the impedances of the junction at the corresponding frequencies whereas the off-diagonal elements give the non-linearity necessary for mixing. The matrix elements can be calculated by including small signals at the USB and IF in the RSJ model pumped by the LO signal. The thermal noise is included in the model by the addition of an uncorrelated Gaussian distributed random current fluctuation of variance $\sigma^2 = \Gamma/\Delta\tau$, where $\Gamma = 2ek_B T/\hbar I_c$ is the dimensionless RSJ noise parameter and $\Delta\tau$ is the normalised time step. The matrix is calculated for each value of the bias current and averaged over many realisations of the matrix to take into account the thermal noise. In order to determine the conversion efficiency, we introduce the external part of the circuit described by the diagonal impedance matrix Z_{ext} whose elements Z_u , Z_l and Z_0 are connected to the mixer inputs. Here Z_u and Z_l represent the impedance of the spiral antenna (80Ω) and are taken to be identical. Z_0 is the 50Ω impedance of the microwave readout line. The conversion efficiency is defined as the ratio of the IF power dissipated in the impedance Z_0 to the available test signal power on Z_u (or Z_l). It can be derived from the conversion matrix[17]

$$\eta_c = 4 * \Re(Z_u)\Re(Z_0)|Y_{0u}|^2 \quad (1)$$

where Y_{0u} is the matrix element of the Y matrix defined by $Y = (Z + Z_{\text{ext}})^{-1}$

As shown in figure 3d, the experimental data are in good agreement with the theoretical calculations derived from the three ports model [17]. In particular, it describes well the crossover from the first regime $f_{\text{LO}} < f_c^{\text{max}}$ to the second regime $f_{\text{LO}} > f_c^{\text{max}}$. For the cases $f_{\text{LO}}=20\text{GHz}$ and 70.5 GHz , the noise parameter Γ was taken to be 0.026 corresponding to a critical current of $100\mu\text{A}$ at 58K . For the case $f_{\text{LO}}=140\text{GHz}$, it was not possible to obtain a quantitative agreement with $\Gamma = 0.026$. The best fit, shown in the figure, was obtained for $\Gamma = 0.06$ indicating that the junction is submitted to an extra noise, equivalent to an effective temperature twice larger than the physical one. The conversion efficiency takes a maximum value of 0.3% at 20GHz and decreases to 0.02% at 140GHz . Its overall weak absolute value is due to the low impedance of the junction (approximately 2Ω) compared to the external impedances Z_u and Z_0 , a problem that could be overcome by modifying the geometry of the junction. In principle, the impedance of the junction could be increased easily up to 20Ω by changing both the width and the thickness of the junction, leading to a much higher conversion efficiency.

Although the ion-irradiated Josephson junction fabricated for this study has a characteristic frequency well below any reasonable estimate of the $\text{YBa}_2\text{Cu}_3\text{O}_7$ gap frequency, several developments can be made to optimize the $I_c R_n$ product [18, 19]. In particular, a higher fluence of irradiation combined with an annealing of the sample should lead to a qualitative improvement [20, 21]. Let us also mention that junctions made recently by irradiation through larger slits display f_c values up to 500 GHz (Supplementary Material figure 1). This is a promising result although their

mixing properties have not been measured yet.

In conclusion, we have demonstrated the mixing operation of ion-irradiated $\text{YBa}_2\text{Cu}_3\text{O}_7$ Josephson junctions up to 140 GHz at 58K in good agreement with the three ports RSJ model. In particular, we have clearly shown the transition between two mixing regimes $f_{\text{LO}} < f_c^{\text{max}}$ and $f_{\text{LO}} > f_c^{\text{max}}$. In the short term, characteristic frequencies of order 500 GHz at $T > 40$ K are entirely within reach enabling mixing operation up to ~ 1 THz. In addition, the natural scalability of the ion irradiation technique [13] makes it particularly interesting to implement, next to the mixer, an integrated Josephson local oscillator made of a large number of junctions and whose frequency could be tuned by dc biasing [22, 23].

The authors thank L. Olanier for technical support. This work was supported by the international cooperation program MINCyT-ECOS A10E05, the Emergence program Contract of Ville de Paris and by the Région Ile-de-France in the framework of CNano IdF and Sesame program and by the PEPS NANANA of CNRS. CNano IdF is the nanoscience competence center of Paris Region, supported by CNRS, CEA, MESR and Région Ile-de-France.

-
- [1] M. Tonouchi, *Nature Photonics* **1**, 97-105 (2007).
 - [2] T. De Graauw, F. P. Helmich, T.G. Phillips, J. Stutzki, E. Caux, N. D. Whyborn, P. Dieleman, P. R. Roelfsema, H.Aarts, R. Assendorp et al., *A&A* **518**, L6 (2010).
 - [3] C. A. Mears, Q. Hu, P. L. Richards, A. H. Worsham, D. E. Prober and A. V. Räisänen, *Appl. Phys. Lett.* **57**, 2487-2489 (1990).
 - [4] R.J. Schoelkopf. PhD thesis, California Institute of Technology, Pasadena, (1995).
 - [5] J. H. Claassen and P. L. Richards, *J. Appl. Phys.*, **49**, 4117, (1978).
 - [6] J. Scherbel, M. Darula, O. Harnack, M. Siegel, *IEEE Trans. Appl. Supercon.* **12**, 1828 (2002).
 - [7] O. Harnack, M. Darula, S. Beuven, and H. Kohlstedt. *Appl. Phys. Lett.*, **76**, 1764 (2000).
 - [8] M. Tarasov, E. Stepantsov, D. Golubev, Z. Ivanov, T. Claeson, O. Harnack, M. Darula, S. Beuven, H. Kohlstedt, *IEEE Trans. Appl. Supercond.* **9**, 3761-3764, (1999).
 - [9] N. Bergeal, X. Grison, J. Lesueur, G. Faini, M. Aprili, J.P. Contour, *App. Phys. Lett.* **87**, 102502 (2005).
 - [10] F. Kahlmann, A. Engelhardt, J. Schubert, W. Zander, C. Buchal, J. Hollkott, *Appl. Phys. Lett.* **73**, 2354-2356 (1998).
 - [11] N. Bergeal, J. Lesueur, G. Faini, M. Aprili, J-P. Contour, *App. Phys. Lett.* **93**, 182502 (2008).
 - [12] S.A. Cybart, S. M. Wu, S. M. Anton, I. Siddiqi, J. Clarke, R. C. Dynes, *App. Phys. Lett* **89**, 112515 (2006).

- [13] S. A. Cybart, S. M. Anton, S. M. Wu, J. Clarke, R. C. Dynes, *Nano Lett.* **9**, 3581 (2009).
- [14] N. Bergeal, J. Lesueur, M. Sirena, G. Faini, M. Aprili, J-P. Contour, B. Leridon, *J. App. Phys* **102**, 083903 (2007).
- [15] D. E. McCumber, *J. App. Phys.* **39**, 3113 (1968).
- [16] S. Shapiro, *Phys. Rev. Lett.*, **11**, 80 (1963).
- [17] Y. Taur, *IEEE T Electron Dev*, 27(10):19211928, (1980)
- [18] M. Sirena, X. Fabreges, N. Bergeal, J. Lesueur, G. Faini, R. Bernard, J. Briatico, *App. Phys. Lett* **91** 262508 (2007).
- [19] M. Sirena, S. Matzen, N. Bergeal, J. Lesueur, G. Faini, R. Bernard, J. Briatico, D. G. Crete, J. P. Contour, *J. App. Phys.* **101**, 123925 (2007).
- [20] M. Sirena, S. Matzen, N. Bergeal, J. Lesueur, G. Faini, R. Bernard, J. Briatico, D. G. Crete, J. P. Contour, *App. Phys. Lett.* **114**, 142506 (2007).
- [21] M. Sirena, S. Matzen, N. Bergeal, J. Lesueur, G. Faini, R. Bernard, J. Briatico, D. G. Crete, *J. App. Phys.* **105**, 023910 (2009).
- [22] P. Barbara, A.B. Cawthorne, S.V. Shitov, C.J. Lobb, *Phys. Rev. Lett.* **82**, 1963 (1999).
- [23] Darula, M. Darula, T. Doderer, S. Beuven, *Supercond. Sci. Technol.* **12** R1R25 (1999).

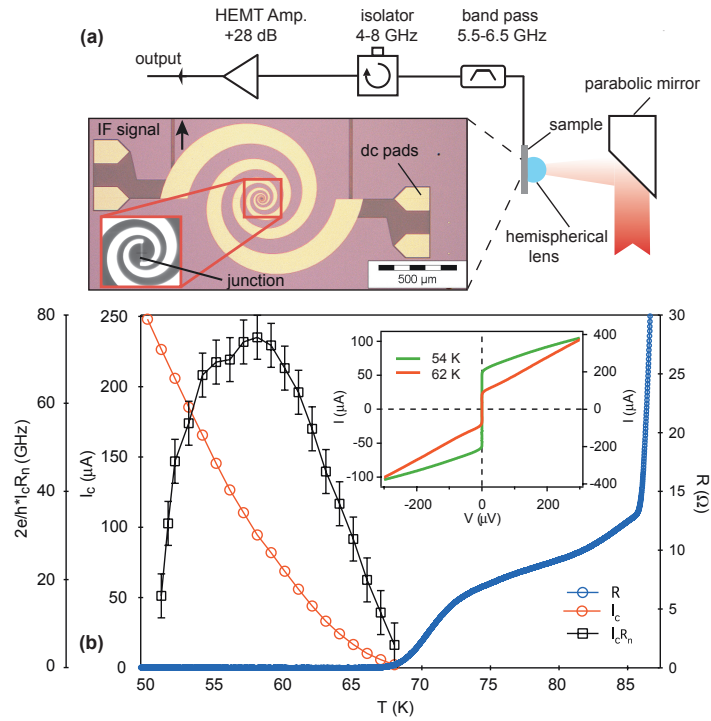


FIG. 1: a) Josephson mixer in its optical and microwave set-up. The junction is embedded in a wide-band spiral antenna (85 GHz - 7 THz). b) Resistance, critical current and $I_c R_n$ product of the junction as a function of temperature. Inset) $I(V)$ curves at two temperatures below and above T'_c showing the difference between the Josephson regime (upward curvature) and the flux flow regime (downward curvature).

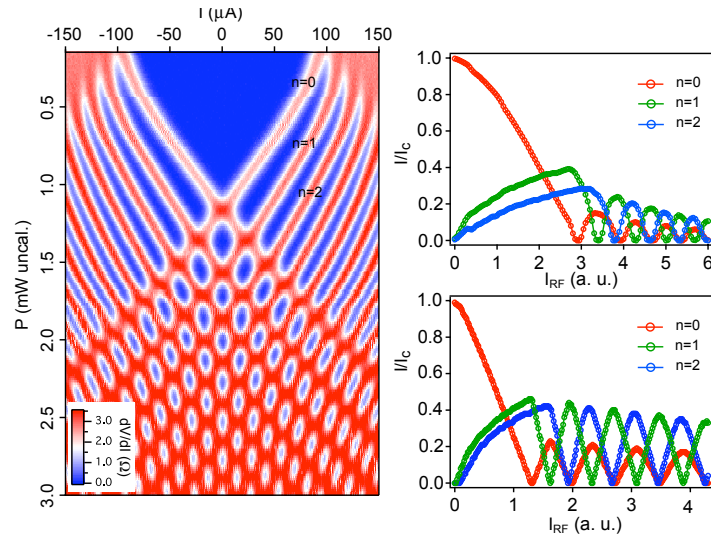


FIG. 2: a) Differential resistance of junction (color scale) under a 20 GHz signal as function of bias current and signal power. b) Experimental height of the $n=0$, $n=1$ and $n=2$ Shapiro steps as a function of signal current measured at $T=58\text{K}$. c) Theoretical height of the $n=0$, $n=1$ and $n=2$ Shapiro steps as a function of signal current obtained from the RSJ model.

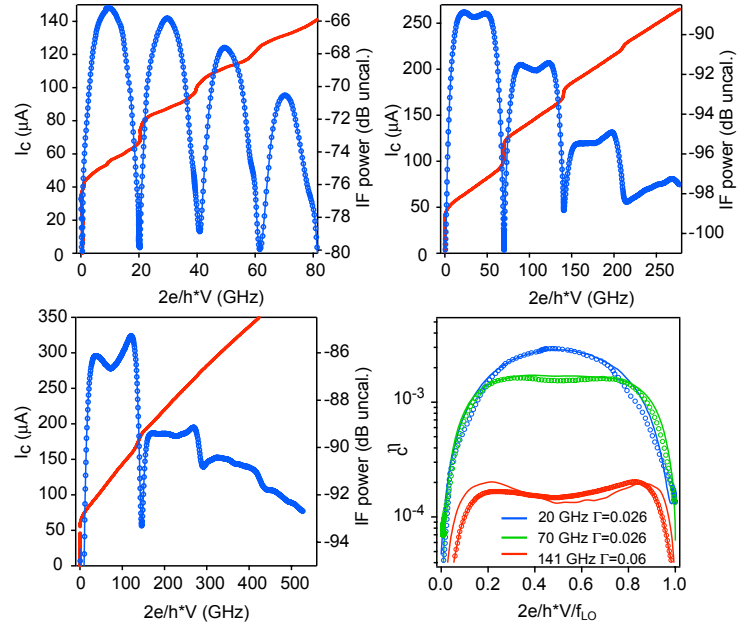


FIG. 3: : a,b,c) Output power at the intermediate frequency (right scale) and dc current (left scale) as function of voltage for three different frequencies : a) $f_{LO}=20\text{GHz}$ and $f_s=14.5\text{GHz}$; b) $f_{LO}=70.5\text{GHz}$ and $f_s=76\text{GHz}$ and c) $f_{LO} = 140\text{GHz}$ and $f_s=145.5\text{GHz}$. The power of the signal has been set to approximatively one thousandth of the power of the local oscillator. d) Comparison between experimental (dots) and theoretical (full lines) conversion efficiency η_C . The noise parameter Γ used for the calculation is indicated on the figure.

Supplementary Material

Irradiation through slits of different widths

The junction presented in the article is defined in a $2\ \mu\text{m}$ wide, 70nm thick, $\text{YBa}_2\text{Cu}_3\text{O}_7$ superconducting channel by irradiating through a 20nm wide slit with 100keV oxygen ions at a fluence of $3 \times 10^{13}\ \text{at}/\text{cm}^2$. We have also made junction irradiated through $30\ \text{nm}$, $40\ \text{nm}$ and $100\ \text{nm}$ wide slits. Supplementary figure 1 shows that these junctions exhibit a higher $I_c R_n$ product. In particular, junction irradiated through a $100\ \text{nm}$ slit has a maximum characteristic frequency of approximately $500\ \text{GHz}$, which should enable mixing operation up to 1THz at temperature around 40K . In addition, these junctions have a higher resistance R_n and are therefore easier to match with the antenna and readout circuit impedances.

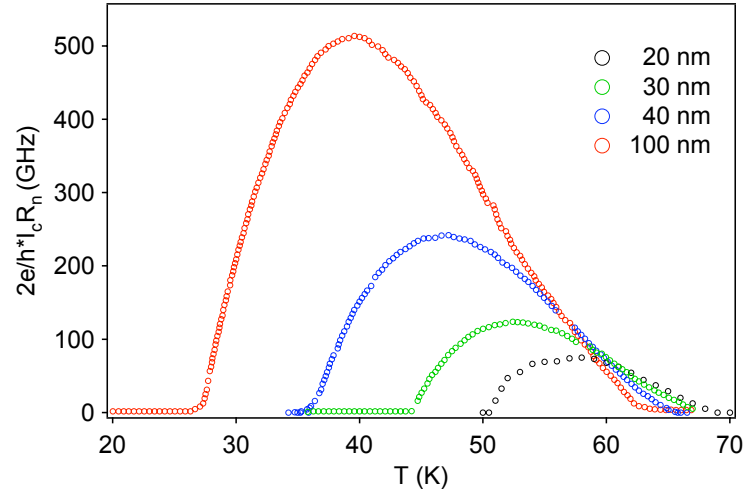


FIG. 4: $I_c R_n$ product as a function of temperature for junctions irradiated through different widths of the slit.